Kinetics of the $C_2H_3 + H_2 \rightleftarrows H + C_2H_4$ and $CH_3 + H_2 \rightleftarrows H + CH_4$ Reactions

Vadim D. Knyazev,* Ákos Bencsura,† Stanislav I. Stoliarov, and Irene R. Slagle*

Department of Chemistry, The Catholic University of America, Washington, DC 20064

Received: February 29, 1996; In Final Form: April 18, 1996[⊗]

The kinetics of the reactions $C_2H_3 + H_2 \rightarrow H + C_2H_4$ (1) and $CH_3 + H_2 \rightarrow H + CH_4$ (2) have been studied in the temperature ranges 499−947 K (reaction 1) and 646−1104 K (reaction 2) and He densities (6−18) × 10^{16} atoms cm^{-3} by laser photolysis/photoionization mass spectrometry. Rate constants were determined in time-resolved experiments as a function of temperature. Ethylene was detected as a primary product of reaction 1. Within the above temperature ranges the experimental rate constants can be represented by Arrhenius expressions $k_1 = (3.42 \pm 0.35) \times 10^{-12} \exp(-(4179 \pm 67\ \text{K})/T)$ cm^3 $molecule^{-1}$ s^{-1} and $k_2 = (1.45 \pm 0.18) \times 10^{-11} \exp(-(6810 \pm 102\ \text{K})/T)$ cm^3 $molecule^{-1}$ s^{-1}. Experimental values of k_2 are in agreement with the available literature data. The potential energy surface and properties of the transition state for reactions (1, −1) were studied by ab initio methods. Experimental and ab initio results of the current study were analyzed and used to create a transition state model of the reaction. The resulting model provides the temperature dependencies of the rate constants for both direct (1) and reverse (−1) reactions in the temperature range 200−3000 K: $k_1 = 1.57 \times 10^{-20} T^{2.56} \exp(-(2529\ \text{K})/T)$ cm^3 $molecule^{-1}$ s^{-1}, $k_{-1} = 8.42 \times 10^{-17} T^{1.93} \exp(-(6518\ \text{K})/T)$ cm^3 $molecule^{-1}$ s^{-1}. Data on reactions 1 and −1 available in the literature are analyzed and compared with the results of the current study.

I. Introduction

Vinyl radicals are recognized as important intermediates in hydrocarbon combustion processes with elementary reactions of C_2H_3 influencing both the rate and products of the overall combustion process. The reaction

$$H + C_2H_4 \rightarrow C_2H_3 + H_2 \qquad (-1)$$

is an important source of vinyl radicals in flames.[1] No direct measurements of the rate constant of this reaction are reported in the literature, although several indirect studies[2−5] have been reported over the past 25 years. Yampol'skii[4] and Nametkin et al.[5] studied reaction −1 by final product analysis of C_2H_4 pyrolysis at temperatures 1073−1213 K. Just et al.[2] studied the unimolecular decomposition of ethylene and reaction −1 behind reflected shock waves by applying optical methods for the detection of H atoms and C_2H_4. These authors derived approximate values of k_{-1} at temperatures 1700−2080 K. Jayaweera and Pacey[3] determined the rate constant of reaction −1 by gas chromatographic analysis of the products of ethylene pyrolysis at 900 K.

The kinetics of the reverse reaction,

$$C_2H_3 + H_2 \rightarrow H + C_2H_4 \qquad (1)$$

can be used to obtain information on k_{-1} via the known thermochemistry of reactions (1,−1). Reaction 1 also plays an important role in the modeling of the chemistry of hydrocarbons in the atmospheres of giant planets.[6]

Reaction 1 has been studied by indirect methods only at low temperatures. Callear and Smith[7] investigated reaction 1 at 300 and 400 K by a gas chromatographic product analysis. Although the rate constants reported by these authors are widely cited as experimental results, in fact, only the ratio of the rate constant of reaction 1 at 400 K to that at 300 K was determined experimentally, providing only a measure of activation energy. The ratios of k_1 to the rate constants of the addition of vinyl radicals to acetylene were also determined at these two temperatures.

Fahr et al.[6] obtained the value of the rate constant of reaction 1 at room temperature by using laser photolysis with kinetic absorption spectroscopy and gas chromatographic product analysis. These authors' result ($k_1 = (3 \pm 2) \times 10^{-20}$ cm^3 $molecule^{-1}$ s^{-1}) is 3 orders of magnitude lower than that reported by Callear and Smith.[7]

Mebel et al.[8] studied reaction 1 using various ab initio methods combined with variational transition-state theory. These authors reported several different $k_1(T)$ dependencies obtained by using different theoretical methods. Tsang and Hampson[9] provided recommendations for the temperature dependencies of the rate constants of reactions 1 and −1 based on a bond energy − bond order fit to the data of Just et al.[2] on reaction −1 and the reaction thermochemistry. Baulch et al.[10] recommended somewhat higher k_{-1} values on the basis of an analysis of the available literature data. Laufer et al.[11] applied the bond order − bond energy method to predict the rate constants of reaction 1 at low temperatures, and Weissman and Benson[12] used transition-state theory to calculate k_1 and k_{-1} temperature dependencies.

Here, we report the results of a study of reaction 1 obtained using laser photolysis/photoionization mass spectrometry at temperatures in the range 499−947 K and bath gas (He) densities (6−18) × 10^{16} atoms cm^{-3}. The experiments on reaction 1 required measuring rate constants as low as 8×10^{-16} cm^3 $molecule^{-1}$ s^{-1} and working with concentrations of H_2 as high as 1.07×10^{17} molecules cm^{-3}. Although the experimental technique applied in the current study has been successfully used for measuring rate constants of many reactions of hydrocarbon radicals, including those of vinyl radicals (e.g., refs 13−16 and references cited therein), there have been no prior studies of such slow reactions of free radicals with molecular hydrogen using this technique. In order to confirm the accuracy

† On leave from the Central Research Institute for Chemistry, Hungarian Academy of Sciences, P.O. Box 17, H-1525 Budapest, Hungary.

[⊗] Abstract published in *Advance ACS Abstracts,* June 1, 1996.

S0022-3654(96)00656-9 CCC: $12.00

of the experimental method, we therefore also measured the rate constants of reaction

$$CH_3 + H_2 \rightarrow H + CH_4 \qquad (2)$$

at temperatures 646−1104 K and bath gas (He) densities (6−18) × 10^{16} atoms cm^{-3}. Both reaction 2 and the reverse reaction

$$H + CH_4 \rightarrow CH_3 + H_2 \qquad (-2)$$

have been studied by many groups using a variety of methods (see, for example, reviews in refs 9, 10, 17−19). Rate constants of reaction 2 obtained in our experiments, as well as those of the reverse reaction, −2, calculated from the k_2 values and known thermochemistry, agree well with the results of other groups (see below). Such agreement indicates the absence (in the technique used here) of significant sources of experimental errors associated with measuring low rate constants of $R + H_2$ reactions using high concentrations of molecule hydrogen.

In order to obtain the rate constant values for the reactions 1 and −1, accurate extrapolation to temperatures outside of the range of the current experiments is required. Ab inition and transition-state theory modeling, together with the known thermochemistry of reactions (1,−1), resulted in $k_1(T)$ and $k_{-1}(T)$ rate expressions that allow extrapolation to temperatures other than those of our experiments. Tunneling was included by using a method (applied earlier[15] in this laboratory to the modeling of C_2H_3 unimolecular decomposition) in which an important parameter—the width of the potential energy barrier—is obtained from ab initio calculations.

II. Experimental Study and Results

Vinyl radicals were produced by the pulsed, 193-nm laser photolysis of vinyl bromide[13]

$$C_2H_3Br \xrightarrow{193\ nm} C_2H_3 + Br$$
$$\rightarrow \text{other products} \qquad (3)$$

The decay of C_2H_3 was subsequently monitored in time-resolved experiments using photoionization mass spectrometry. Details of the experimental apparatus used have been described before.[20] In the current experimental setup, a quartz reactor coated with boron oxide was used. Neither the laser intensity nor the concentration of the radical precursor had any observable influence on the kinetics of C_2H_3 radicals. Initial conditions (precursor concentration and laser intensity) were selected to provide low radical concentrations ($\leq 10^{11}$ molecules cm^{-3}) such that reactions between radical products had negligible rates compared to that of the reaction of vinyl radicals with molecular hydrogen.

Experiments were conducted under pseudo-first-order conditions with $[H_2]$ in the range 8.4 × 10^{14} to 1.07 × 10^{17} molecules cm^{-3}. The observed exponential decay of the C_2H_3 radical was attributed to reaction 1 and heterogeneous loss:

$$C_2H_3 \rightarrow \text{heterogeneous loss} \qquad (4)$$

The vinyl ion signal profiles were fit to an exponential function ($[C_2H_3]_t = [C_2H_3]_0 e^{-k't}$, where $k' = k_1[H_2] + k_4$) by using a nonlinear least squares procedure. In a typical experiment to determine k_1, the kinetics of the decay of C_2H_3 radicals was recorded as a function of the concentration of molecular hydrogen. When high concentrations of H_2 were used, that of

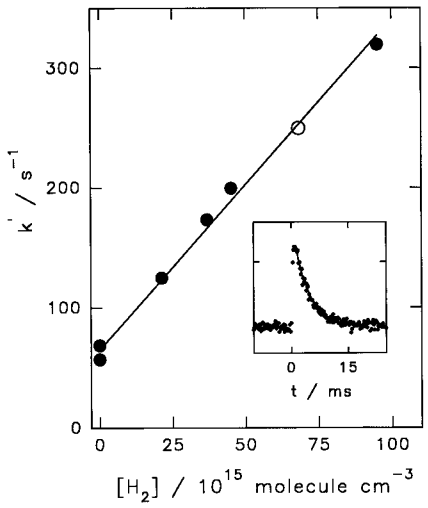

Figure 1. First-order C_2H_3 decay rate k' vs $[H_2]$. The intercept at $[H_2] = 0$ corresponds to the rate of heterogeneous decay of C_2H_3 radicals: $T = 601$ K; $[M] = 18.0 \times 10^{16}$ molecules cm^{-3}; $[C_2H_3Br] = 6.2 \times 10^{11}$ molecules cm^{-3}. The insert shows the recorded C_2H_3 decay profile for the conditions of the open circle: $[H_2] = 6.83 \times 10^{16}$ molecules cm^{-3}; $k' = 249.8 \pm 7.5$ s^{-1}.

He was reduced accordingly so that the total density of gas ([M]) in the reactor remains constant. Values of k_4 were determined in the absence of H_2. Values of k_1 were obtained from the slope of a linear plot of k' vs $[H_2]$. The average value of k'/k_4 achieved with the highest concentrations of H_2 used at each temperature is 4.2. This ratio was, however, necessarily reduced at the higher end of the experimental temperature range due to (1) an increase in k_4 because of a contribution from the thermal decomposition of vinyl radicals and (2) a decrease in the sensitivity of the detection system with increasing temperature, which resulted in greater difficulty in measuring k' values above 250 s^{-1}. Experiments were performed to establish that the decay constants did not depend on the initial C_2H_3 concentration (provided that the concentration was kept low enough to ensure that radical−radical reactions had negligible rates in comparison to the reaction with H_2), the concentration of the radical precursor or the laser intensity. Rate constants of reaction 1 were determined at $T = 499-947$ K and $[M] = (6-18) \times 10^{16}$ atoms cm^{-3}. An example of a k' vs $[H_2]$ plot is shown in Figure 1. The intercept at $[H_2] = 0$ corresponds to the rate of heterogeneous decay of C_2H_3 radicals, k_4. Ethylene was detected as a product of reaction 1 with its rise time matching that of C_2H_3 exponential decay due to reaction 1.

Rate constants of the heterogeneous loss of vinyl radicals, k_4, depend on the quality of the wall coating which, in turn, depends on the history of exposure to the reaction environment. At the highest temperatures used the "effective" k_4 also included a contribution from thermal decomposition of the C_2H_3 radical (Table 1), which determined the upper temperature limit of the experiments. The observed linear dependence of k' on $[H_2]$ ($k' = k_1[H_2] + k_4$) is in agreement with the assumed first-order nature of the heterogeneous reaction 4.

In many earlier studies of reactions of hydrocarbon radicals (including C_2H_3) with stable molecular reactants conducted by the same experimental technique as used here, the contribution of a potential bimolecular heterogeneous reaction was ruled out by using different coating materials (e.g., ref 14). In these studies, determinations of the $R + reactant$ rate constants conducted with different wall coatings yielded different heterogeneous decay rates (equivalents of k_4) but identical bimolecular gas-phase reaction rate constants. In the current study,

TABLE 1: Conditions and Results of Experiments To Measure k_1

T/K	[M]/(10^{16} atoms cm^{-3})	[C_2H_3Br]/(10^{11} molecules cm^{-3})	I^a	[H_2]/(10^{15} molecules cm^{-3})	k_4/s^{-1}	$k_1{}^b$/(10^{-14} cm^3 molecule^{-1} s^{-1})
499	18.0	6.1	10	36.5−107.4[c]	35.0	0.082 ± 0.008
499	18.0	6.1	4.1	36.5−107.4[c]	26.8	0.081 ± 0.011
500	18.0	5.0	8.9	38.0−105.3	42.7	0.081 ± 0.012
549	18.0	5.7	5.1	23.6−83.6	97.7	0.175 ± 0.030
600	18.0	16.6	8.9	23.1−78.5	79.9	0.325 ± 0.040
600	18.0	16.6	3.5	23.1−44.4	80.1	0.390 ± 0.051
601	18.0	6.2	10	21.3−95.2	62.8	0.280 ± 0.030
650	18.0	5.6	13	9.96−39.7	87.0	0.522 ± 0.060
650	6.0	3.09	28	11.8−30.7[c]	44.2	0.544 ± 0.064
700	18.0	6.0	8.9	5.50−36.4	37.2	0.818 ± 0.089
700	18.0	6.0	3.5	5.50−26.1	27.2	0.820 ± 0.105
747	18.0	6.1	14	3.29−10.75	64.8	1.24 ± 0.15
747	18.0	6.1	5.6	3.38−9.99	62.5	1.20 ± 0.16
850	18.0	5.0	5.1	1.33−5.28[c]	34.9	2.54 ± 0.35
851	18.0	5.8	4.6	2.36−6.60	55.9	2.43 ± 0.28
939	6.1	5.7	21	0.836−2.92	103.3[d]	4.70 ± 0.52
947	6.0	5.4	12	0.890−3.00	107.8[d]	4.20 ± 0.65

[a] Photolyzing laser intensity (mJ cm^{-2} pulse^{-1}). [b] All error limits are 1σ with uncertainties in [$H]_2$ included. [c] Research Grade H_2 (99.9995%, Air Products) was used. [d] Includes contribution from thermal decomposition.

TABLE 2: Conditions and Results of Experiments To Measure k_2

T/K	[M]/(10^{16} atoms cm^{-3})	[$(CH_3)_2CO$]/(10^{11} molecules cm^{-3})	I^a	[H_2]/(10^{15} molecules cm^{-3})	$k_{wall}{}^b$/s^{-1}	$k_1{}^c$/(10^{-15} cm^3 molecule^{-1} s^{-1})
646	18.0	15.5	35	43−140	12	0.404 ± 0.046
646	18.0	15.5	14	43−140	8	0.407 ± 0.042
699	18.0	9.0	40	34−95	13	0.842 ± 0.101
751	18.0	29.0	10	18−78	7	1.62 ± 0.19
751	18.0	29.0	40	18−78	13	1.57 ± 0.17
820	6.0	32.0	20	6.7−32	9	3.50 ± 0.37
904	18.0	15.2	40	4.3−13	5	7.21 ± 0.73
1000	18.0	8.9	30	2.3−8.5	7	15.7 ± 1.7
1000	18.0	30.2	30	2.4−8.2	5	14.2 ± 1.5
1104	6.0	19.7	30	0.74−6.0	10	32.0 ± 3.4
1104	6.0	19.7	12	0.74−6.0	11	35.2 ± 3.8

[a] Photolyzing laser intensity (mJ cm^{-2} pulse^{-1}). [b] Rate constant of CH_3 wall reaction. [c] All error limits are 1σ with uncertainties in [$H]_2$ included.

high experimental temperatures precluded the use of any wall coating material other than boron oxide, and, therefore, a similar investigation of potential second-order heterogeneous effects could not be performed. The agreement of our earlier results on the kinetics of $C_2H_3 + O_2$ reaction (ref 13 and references cited therein) and of our current results on $CH_3 + H_2$ with the literature data (see below) indicates the absence of any such heterogeneous effects in the cases of these two reactions. While not being a rigorous proof, this leads us to expect no significant contributions from a second-order heterogeneous reaction in the $C_2H_3 + H_2$ system.

Rate constants of reaction 2 were similarly determined at temperatures 646−1104 K and bath gas (He) densities (6−18) × 10^{16} molecules cm^{-3}. Photolysis of acetone at 193 nm was used as a source of CH_3 radicals. Variation of laser intensity and the precursor concentration did not affect the values of k_2 obtained.

The gases used were obtained from Aldrich (acetone, 99.9%) and Matheson (He, >99.995%; H_2, >99.99%; C_2H_3Br, 99.5%). Precursors were purified by vacuum distillation prior to use. Helium and hydrogen were used as provided. In order to eliminate a possible influence of a minor impurity in hydrogen on the measured rate constants, several experiments on reaction 1 were performed using Research Grade H_2 (99.9995%) obtained from Air Products. No effect of the nominal purity of the hydrogen used on the values of k_1 could be detected. The sources of ionizing radiation were hydrogen (10.2 eV, MgF_2 window, used for the detection of C_2H_3 and CH_3 radicals) and Ar (11.6−11.9 eV, LiF window, used for the detection of ethylene) resonance lamps.

The values of the bimolecular rate constants k_1 and k_2 determined in this study are presented in Tables 1 and 2 and on Arrhenius plots in Figures 2 and 3. The results of the current study yield the Arrhenius expressions:

$$k_1 = (3.42 \pm 0.35) \times 10^{-12} \exp(-(4179 \pm 67\ \mathrm{K})/T)\ \mathrm{cm^3\ molecule^{-1}\ s^{-1}} \quad \text{at } T = 499-947\ \mathrm{K}$$

$$k_2 = (1.45 \pm 0.18) \times 10^{-11} \exp(-(6810 \pm 102\ \mathrm{K})/T)\ \mathrm{cm^3\ molecule^{-1}\ s^{-1}} \quad \text{at } T = 646-1104\ \mathrm{K}$$

III. Data Analysis for Reactions (1,−1)

In this section we present the development of a model of reactions (1,−1) which describes both our experimental data on reaction 1 and permits extrapolation of k_1 and k_{-1} values to temperatures outside the experimental range. Properties of the $C_2H_3-H_2$ transition state (including the width of the potential energy barrier—a parameter important in the treatment of tunneling) are determined from an ab initio study. These ab initio results are used in a model of reactions (1,−1), the parameters of which (energy barrier and lowest vibrational frequencies of the transition state) are adjusted to reproduce the experimental data. Rate constant values for reaction −1 are obtained from those for reaction 1 via equilibrium constants calculated from the known thermochemistry. The uncertainties of the extrapolation of rate constants to other temperatures are evaluated.

III.1. Ab Initio Study of the Transition State of Reactions (1,−1) and the Shape of the Potential Energy Profile Along the Reaction Path. The geometries and harmonic vibrational frequencies of the $C_2H_3-H_2$ transition state ($C_2H_3-H_2^{\ddagger}$) were studied using the ab initio UMP2 method with the 6-31G** basis. Energies were calculated with the UMP4/6-31G** and

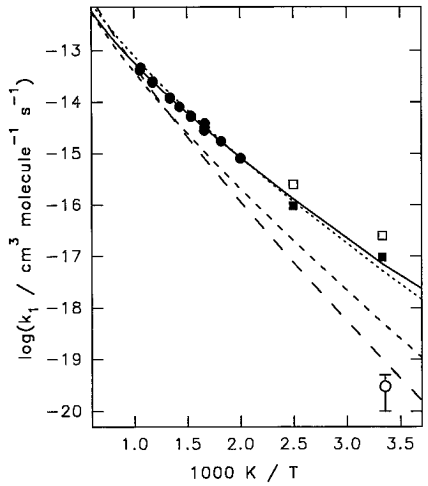

Figure 2. Plot of experimental and calculated rate constants (k_1) of the reaction of C_2H_3 radicals with H_2 vs temperature. Experimental data: (closed circles) current study; (open squares) ref 7 (as reported); (closed squares) ref 7 shifted to agree with the results of the current study (see text); (open circle) ref 6. Calculations: (solid line) current model (formula IV); (long dash) ref 9; (medium dash) ref 8; (short dash) ref 8 with the energy barrier changed by −5.8 kJ mol^{-1} (see text).

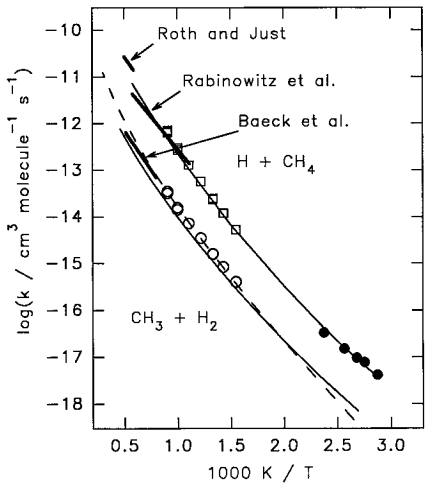

Figure 3. Plot of the rate constants of reactions 2 and −2. Experimental data: (open circles) k_2 values of the current study; (open squares) the same data converted to k_{-2} values; (closed circles) k_{-2} values from Marquaire et al.;[18] (heavy lines) k_2 from Baeck et al.[19] and k_{-2} from Roth and Just[21] and Rabinowitz et al.[17] Calculated values (thin lines): (solid lines) k_2 and k_{-2} from Marquaire et al.;[18] (dashed line) recommendation on k_2 from Baulch et al.[10]

PMP4/6-31G** methods. For the purpose of obtaining complete information on the shape of the potential energy surface along the reaction coordinate, properties of H_2 and ethylene were also calculated at different levels of theory. Properties of the vinyl radical were taken from ref 15. Structures and energies of these species are listed in Table 3. The GAUSSIAN 92 system of programs[22] was used in all ab initio calculations.

The shape of the potential energy barrier for reactions (1,−1) was calculated using the method of reaction path following in mass-weighted internal coordinates described by Gonzalez and Schlegel.[23] For each point along the reaction path, optimization was done at the UMP2/6-31G** level and energy was calculated at the UMP4/6-31G** level. Spin contamination was removed by the spin projection (PMP4) method of Schlegel.[24,25]

The results of this ab initio study of the transition state $C_2H_3-H_2^{\ddagger}$ and the reaction path were used in creating a model of reactions (1,−1). Although the reaction energy threshold values calculated at the applied levels of theory are not believed to be sufficiently accurate, the geometrical configuration of the transition state (Table 3) was used in the model. The calculated set of vibrational frequencies of the transition state (scaled[26] by 0.94, Table 3) was used as a basis for the model. These frequencies, as expected, are very close to those obtained by Mebel et al.[8] at the UMP2/6-31G* level with the QCISD(T)/6-311** geometry optimization.

TABLE 3: Geometrical Structure[a] and Energies of C_2H_3, $C_2H_3-H_2^{\ddagger}$, C_2H_4, and H_2 Obtained in the Ab Initio Study

property	C_2H_3[b]	$C_2H_3-H_2^{\ddagger}$[c]	C_2H_4	H_2
Bond Distances (Å) and Bond Angles (deg)				
C1C2	1.288	1.290	1.335	
H11C1	1.086	1.082	1.081	
H12C1	1.082	1.084	1.081	
H21C2	1.077	1.080	1.081	
H22C2		1.444	1.081	
H11C1C2	121.63	121.85	121.57	
H12C1C2	122.05	121.55	121.57	
H21C2C1	136.41	131.54	121.57	
H22C2C1		115.70	121.57	
H5H22		0.8483		0.7340
H5H22C2		175.58[d]		
Energies (hartrees)				
E(HF/6-31G**)	−77.394 251	−78.487 172	−78.038 334	−1.131 332
E(MP2/6-31G**)	−77.627 982	−78.768 569	−78.317 282	−1.157 661
E(MP4/6-31G**)	−77.663 531	−78.810 649	−78.353 792	−1.164 566
E(PMP4/6-31G**)	−77.671 223	−78.819 911		

[a] C_2H_3, $C_2H_3-H_2^{\ddagger}$, and C_2H_4 have planar structure. [b] Data for C_2H_3 taken from ref 15. [c] UMP2/6-31G** vibrational frequencies (scaled by 0.94) are 3129, 3119, 3031, 2061, 1800, 1387, 1144, 1077, 1037, 993, 968, 810, 374, 274, and 1449*i*. [d] The H5−H22 bond bends toward the C−C bond.

The shapes of the potential energy surface obtained at different levels of calculations (UMP2, UMP4, and PMP4) were used to determine the width of the potential energy barrier—an important parameter required for the modeling of tunneling. The potential energy profile along the reaction path was fitted with the Eckart function

$$V = \frac{A\xi}{1+\xi} + \frac{B\xi}{(1+\xi)^2};\quad \xi = \exp\left(\frac{2\pi x}{l}\right) \qquad \text{(I)}$$

where x is a coordinate along the reaction path, l is a parameter determining the width of the barrier, and parameters A and B are related to the barriers for the direct and reverse reactions E_1 and E_{-1}:

$$A = \Delta E_{1,-1} = E_1 - E_{-1};\quad B = (E_1^{1/2} + E_{-1}^{1/2})^2 \qquad \text{(II)}$$

The transition probability for such a barrier can be described analytically, as shown by Eckart.[27] In the fitting process, parameter A was fixed at the value obtained from ab initio calculations, and B and l were determined from the fitting. Only points with energy above that of $C_2H_3 + H_2$ were used (Figure 4). The resultant values of B, l, and E_{-1} are listed in Table 4 for three levels of calculations used. Although it can clearly be seen that improvement of the level of theory results in a significant reduction of the reverse reaction barrier, the barrier width changes only slightly—from 1.64 amu$^{1/2}$ Å at the UMP2 level to 1.60 amu$^{1/2}$ Å at the UMP4 level and to 1.64 amu$^{1/2}$ Å at the PMP4 level. In the model of reactions (1,−1) we use the PMP4 value.

III.2. Transition State Model of Reactions (1,−1). The physical properties of C_2H_4 and H_2 are well-known.[28−30] For the vinyl radical, we use the set of frequencies and rotational constants reported by Ervin et al.[31] which is a combination of experimental measurements and ab initio calculations. Properties of the $C_2H_3-H_2^{\ddagger}$ transition state were obtained from our

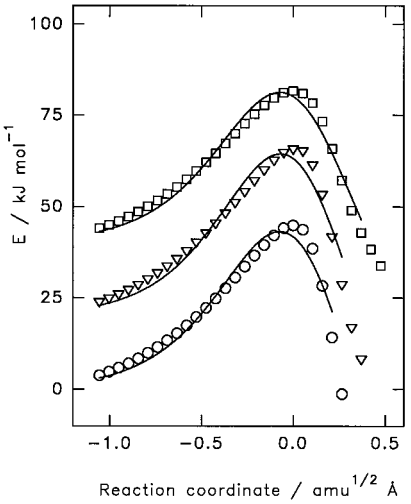

Figure 4. Shapes of potential energy barrier of reactions (1,−1) obtained at different levels of calculation: (Circles) UMP2; (triangles) UMP4; (squares) PMP4. Data obtained at each next level of calculations are shifted upward by 20 kJ mol^{-1}. Lines represent fits to Eckart function. Energy relative to $C_2H_3 + H_2$.

TABLE 4: Eckart Parameters Obtained from Fitting the Potential Energy Profile Along the Reaction Path

	UMP2	UMP4	PMP4
A^a/(kJ mol^{-1})	78.4	62.8	42.6
B/(kJ mol^{-1})	309.5	290.0	243.0
l/(amu$^{1/2}$ Å)	1.64	1.60	1.64
$\nu_i{}^b$/cm^{-1}	1184i	1195i	1087i
$E_{-1}{}^b$/(kJ mol^{-1})	43.1	44.5	41.3

[a] A was fixed at the value obtained from ab initio energies of C_2H_3, C_2H_4, H_2, and H. [b] Imaginary frequency ν_i and potential barrier for reaction −1 calculated from the fitted values of B and l.

ab initio study with some of its parameters adjusted to achieve agreement with the experimental results.

Calculation of k_1 and k_{-1} requires knowledge of the thermochemistry of reaction. In this study, we use $\Delta H_f^\circ{}_{298}(H) = 218.0$ kJ mol^{-1} [29] and $\Delta H_f^\circ{}_{298}(C_2H_4) = 52.5 \pm 0.3$ kJ mol^{-1}.[29,30] The heat of formation of the vinyl radical has been a subject of controversy (see reviews in refs 31 and 32). $\Delta H_f^\circ{}_{298}(C_2H_3) = 300.0 \pm 3.3$ kJ mol^{-1}, a value obtained using a method based on gas-phase acidity,[31] is believed[32] to be the most accurate. This value is supported by the results obtained in G2 ab initio calculations,[33a] in modeling[15] of the C_2H_3 decomposition reaction, and in a recent study of the $Cl + C_2H_4$ reaction.[33b] Molecular properties (moments of inertia and vibrational frequencies) of C_2H_3, C_2H_4, and H_2 were taken from Ervin et al.,[31] Chao and Zwolinski,[28] and JANAF Tables,[29] respectively. These data result in the heat of reaction $\Delta H^\circ_{298}(1,-1) = -29.5 \pm 3.6$ kJ mol^{-1} and $\Delta E_{1,-1} = E_1 - E_{-1} = -27.3 \pm 3.6$ kJ mol^{-1}. Here, E_1 and E_{-1} are the energy barriers for the direct (1) and reverse (−1) reactions, respectively.

k_1 is given by[34]

$$k_1(T) = \frac{k_B T}{h} \frac{\kappa(T) Q^\ddagger}{Q_{C_2H_3} Q_{H_2}} \exp\left(-\frac{E_1}{k_B T}\right) \qquad \text{(III)}$$

where $Q^\ddagger$, $Q_{C_2H_3}$, and Q_{H_2} are partition functions of the transition state, vinyl radical, and H_2 molecule, respectively, and $\kappa(T)$ is the temperature-dependent tunneling factor:

$$\kappa(T) = \int_{-E_1}^{\infty} P'(E) e^{-E/k_B T} \, dE$$

Here, $P'(E)$ is the first derivative of the energy-dependent tunneling transition probability $P(E)$. It was calculated using the Eckart formula[27] with the Eckart potential parameters obtained from our ab initio study (barrier width parameter, see section III.1), known $\Delta E_{1,-1}$, and the reaction energy barrier E_1.

TABLE 5: Models of the Molecules and Transition State Used in the Data Analysis

Energy Barriers

$E_1 = 35.8$ kJ mol^{-1} $E_{-1} = 63.0$ kJ mol^{-1} $\Delta E_{1,-1} = -27.2$ kJ mol^{-1}

Vibrational Frequencies (cm^{-1})

C_2H_3:[a]	3265, 3190, 3115, 1670, 1445, 1185, 920, 825, 785
$C_2H_3-H_2^\ddagger$:[b]	3129, 3119, 3031, 2061, 1800, 1387, 1144, 1077, 1037, 993, 968, 810, 508, 372, 981i
C_2H_4:[c]	3026, 3106, 3103, 2989, 1623, 1444, 1342, 1236, 1023, 949, 943, 826
H_2:[d]	4162

Rotational Constants (cm^{-1}) and Symmetry Numbers

C_2H_3:[a]	1.953(1)	C_2H_4:[c]	1.592(4)
$C_2H_3-H_2^\ddagger$:[b]	1.076(1)	H_2:[d]	59.34(2)

[a] Properties of C_2H_3 from ref 31. [b] Structure and vibrational frequencies of $C_2H_3-H_2^\ddagger$ from our ab initio study (two lowest frequencies adjusted). Imaginary frequency calculated from the Eckart potential parameters of the model. [c] Ethylene parameters from ref 28. [d] Properties of H_2 from ref 29.

In the current treatment of tunneling, the barrier width (a geometrical parameter) is determined from ab initio calculations. The imaginary frequency is determined by the width and the height of the reaction barrier. Ab initio UHF and UMP2 methods usually overestimate the barrier height and, therefore, overestimate the curvature of the potential energy surface in the direction of the reaction coordinate and the imaginary frequency associated with the barrier. On the other hand, geometrical parameters are usually determined more accurately by the same methods. This makes the current method of the treatment of tunneling more accurate compared to the one where the imaginary frequency of the transition state obtained from ab initio calculations is used directly in determining the transition probability.

The experimental values of k_1 presented in Table 1 were reproduced by calculations using formula III. The two lowest frequencies of the transition state and E_1 were adjusted to achieve a good fit. The resultant optimized value of E_1 is 35.8 kJ mol^{-1}. The sum of squares of deviations between the experimental and the calculated rate constants was determined as a function of E_1 (E_1 was fixed at some values and the frequencies of the transition state were optimized). From the curvature of this dependence the uncertainty of E_1 was estimated[35] as ±0.8 kJ mol^{-1} (2σ). The fixed and optimized parameters of the model are listed in Table 5.

The optimized model of reactions (1,−1) results in the following expressions for the temperature dependencies of the rate constants of reactions 1 and −1:

$$k_1 = 1.57 \times 10^{-20} T^{2.56} \times \exp(-(2529 \text{ K})/T) \text{ cm}^3 \text{ molecule}^{-1} \text{ s}^{-1} \qquad \text{(IV)}$$

$$k_{-1} = 8.42 \times 10^{-17} T^{1.93} \times \exp(-(6518 \text{ K})/T) \text{ cm}^3 \text{ molecule}^{-1} \text{ s}^{-1} \qquad \text{(V)}$$

at 200 K ≤ T ≤ 3000 K. These modified Arrhenius expressions provide a good fit to the calculated rate constants within the temperature range between 300 and 3000 K—the average deviation is 2% with a maximum deviation of 5%. At lower temperatures the deviation is higher—up to 22% at 200 K. The significant temperature dependence of the preexponential factor of reaction 1 is similar to that predicted by Tsang and Hampson[9] on the basis of a bond energy−bond order analysis.

The uncertainty of these formulas which provide the extrapolation of our experimental data to higher and lower temperatures is determined by three factors. First is the scatter of experimental points which results in error limits for the energy barrier $E_1 \pm 0.8$ kJ mol^{-1} (2σ). Second is the uncertainty resulting from the treatment of tunneling. Third is the additional uncertainty factor for the rate constant of the reaction of H atoms with ethylene resulting from the uncertainties in the enthalpy of reactions (1,−1).

Among these three factors, the most difficult one to estimate is that related to the treatment of tunneling. Unfortunately, the current treatment of tunneling as a one-dimensional motion with an Eckart potential is only a crude approximation. Better methods require detailed knowledge of the potential energy surface, which is not readily available at the current level of theory. In the absence of any rigorous method of calculating potential errors associated with the current treatment of tunneling, we choose to investigate those resulting from changing the most important parameter for the treatment of tunneling—the barrier width l—by a factor of 1.5. The fitting of our experimental results on the rate constant of the reaction of vinyl radicals with H_2 was repeated with the barrier width parameter l increased or reduced by this factor. Reduction of l resulted in a more significant change of E_1 (by +2.8 kJ mol^{-1}) than the increase (by −1.1 kJ mol^{-1}). The resultant modified models of reactions (1,−1) were used to calculate rate constants at temperatures between 200 and 3000 K, and "tunneling" uncertainty factors were obtained from the comparison of these rate constants with those obtained with the unmodified (Table 5) model. The overall uncertainty factors were obtained by including additional factors resulting from the uncertainty in E_1 due to the data scattering and from the uncertainty in $\Delta E_{1,-1}$ (for reaction −1). The resultant overall uncertainty factors f_1 (for reaction 1) and f_{-1} (for reaction −1) are (listed as f_1/f_{-1}) as follows: 24/220 at 200 K, 2.4/10 at 300 K, 1.3/3.9 at 400 K, 1.2/1.6 at 1500 K, and 1.4/1.6 at 3000 K. Potential errors originating in the treatment of all involved species as combinations of rigid rotors and harmonic oscillators (which are likely to become important at high temperatures) are not included here.

IV. Discussion

IV.1. $CH_3 + H_2 \rightleftarrows H + CH_4$ (2,−2). Both reactions 2 and −2 have been studied by many groups using a variety of experimental methods. Reviews are available in refs 9, 10, and 17−19, and references cited therein. Approximate agreement has been reached between the results of different groups, with the exception of the values of k_{-2} at temperatures above 1700 K, where rate constants recently obtained by Rabinowitz et al.[17] are lower than those of Roth and Just[21] by a factor of 3.5. An earlier controversy due to the disagreement between k_2/k_{-2} values obtained from experimental data and those calculated from the known thermochemistry of the reaction has been recently resolved by Marquaire et al.[18] who studied reaction −2 by the ESR/discharge flow method at temperatures 348−412 K. These authors reproduced their experimental data and those of other groups on reactions 2 and −2 with transition-state-theory modeling to provide k_2 and k_{-2} temperature dependencies consistent with the thermochemistry of reactions (2,−2).

Equilibrium constants of reactions (2,−2) were calculated using the known properties of the species involved. With $\Delta H_f^\circ{}_{298}(CH_3)$[32] = 146.4 ± 0.4 kJ mol^{-1} and $\Delta H_f^\circ{}_{298}(CH_4)$[36] = −74.6 ± 0.3 kJ mol^{-1}, we obtain $\Delta H^\circ{}_{298}(2,-2) = -3.0 \pm 0.7$ kJ mol^{-1} and $\Delta E_{2,-2} = -0.4 \pm 0.7$ kJ mol^{-1}. Models of CH_3, CH_4, and H_2 were taken from JANAF tables,[29] and the rotational partition function of molecular hydrogen was calculated numerically by summation over the rotational states. Experimental data on k_2 determined in the current study were converted via the calculated equilibrium constants to the rate constants of the reverse reaction (−2) of H atoms with methane. The values of k_{-2} obtained in this manner can be represented by the Arrhenius dependence

$$k_{-2} = 2.46 \times 10^{-10} \exp(-(6837\ \mathrm{K})/T)\ \mathrm{cm^3\ molecule^{-1}\ s^{-1}} \quad \text{at } T = 646-1104\ \mathrm{K}$$

Data on k_2 and k_{-2} obtained in the current study are presented in Figure 3 together with the recent experimental results of Baeck et al.[19] and the values calculated from the recommendations of Baulch et al.[10] for k_2 and with those calculated by Marquaire et al.[18] from their model of reactions (2,−2). The data of Roth and Just,[21] Rabinowitz et al.,[17] and Marquaire et al. on k_{-2} are also shown. As can be seen from the plot, our results are in good agreement with these data and predictions, confirming the accuracy of the method used in the current experiments.

IV.2. $C_2H_3 + H_2 \rightleftarrows H + C_2H_4$ (1,−1). Although the literature on reactions 1 and −1 is abundant, no direct measurements of rate constants are available. The current study provides the first set of direct determinations of the rate constants of the reaction of vinyl radical with molecular hydrogen.

$C_2H_3 + H_2 \rightarrow H + C_2H_4$ (1). Callear and Smith[7] investigated reaction 1 at 300 and 400 K. Vinyl radicals were generated by attachment of H atoms from the Hg-photosensitized decomposition of H_2 to acetylene. Reaction products were analyzed by gas chromatography. Although rate constants reported by these authors ($k_1 = 2.5 \times 10^{-17}$ cm^3 molecule^{-1} s^{-1} at 300 K and 2.5×10^{-16} cm^3 molecule^{-1} s^{-1} at 400 K) are widely cited as experimental results, their values were obtained by arbitrarily choosing the values of the optical density of the reaction vessel and of the radical termination rate constant. Only the ratio of the rate constant of reaction 1 at 400 K to that at 300 K was determined experimentally, thus yielding an activation energy of 23 ± 1 kJ mol^{-1}.

Fahr et al.[6] employed laser photolysis with kinetic absorption spectroscopy and gas chromatographic product analysis to obtain the value of the rate constant of reaction 1 at room temperature. These authors' results ($k_1 = (3 \pm 2) \times 10^{-20}$ cm^3 molecule^{-1} s^{-1} from the kinetic absorption spectroscopy experiments and $k_1 \approx 1 \times 10^{-20}$ cm^3 molecule^{-1} s^{-1} from the gas chromatographic product analysis experiments) are 3 orders of magnitude lower those reported by Callear and Smith.[7] Vinyl radicals were generated by excimer laser photolysis of divinyl mercury (in optical absorption experiments) or methyl vinyl ketone (in gas chromatographic experiments). In the kinetic absorption spectroscopy experiments, the formation of 1,3-butadiene (C_4H_6) in the reaction of vinyl−vinyl recombination was monitored. The values of k_1 were obtained from kinetic modeling of the observed temporal behavior of the C_4H_6 signal in the presence and in the absence of H_2. In the gas chromatographic experiments, the rate of reaction 1 was compared with that of reaction 2 ($CH_3 + H_2 \rightarrow H + CH_4$). Vinyl and methyl radicals were simultaneously produced in equal concentrations[37] by the 193-nm laser photolysis of methyl vinyl ketone. The ratio of k_1 to k_2 rate constants was determined by comparing the increase of C_2H_4 yield in the presence of H_2 to that of CH_4.

Our extrapolated rate constant at room temperature ($k_1 = 7.1 \times 10^{-18}$ cm^3 molecule^{-1} s^{-1}, uncertainty factor 2.4) is in significant disagreement with the results of Fahr et al. (Figure 2). The difference exceeds 2 orders of magnitude. Even if no tunneling is taken into account and our experimental rate constants are extrapolated assuming a pure Arrhenius dependence, the disagreement is still at least a factor of 50. In prior

investigations to determine the rate constant for the reaction of vinyl radicals with molecular oxygen, the results[13] obtained using a method and apparatus identical with those in this study were in good agreement with those obtained in optical absorption measurements of Fahr and Laufer.[38] The large disparity between the results in the case of the $C_2H_3 + H_2$ reaction therefore cannot be explained by the difference in the radical source or detection method used.

One possible reason for such disagreement is that neither of the two reaction systems used in ref 6 is sufficiently sensitive to the rate constant of the reaction of vinyl radical with H_2. In the kinetic absorption spectroscopy experiments of Fahr et al.,[6] in which initial concentrations $[C_2H_3]_0 = (2.3-16) \times 10^{14}$ molecules cm^{-3} and $[H_2] \approx 2.3 \times 10^{19}$ molecules cm^{-3}, the kinetics was dominated by the fast (rate constant[37] $= 1.3 \times 10^{-10}$ cm^3 molecule^{-1} s^{-1}) self-reaction of vinyl radicals. The characteristic time of fast C_4H_6 growth due to the vinyl recombination was less than 100 μs and the overall time of the kinetic measurement was 350 μs. If the value of $k_1 = 3 \times 10^{-20}$ cm^3 molecule^{-1} s^{-1} reported by Fahr et al. is used, the first-order effective rate constant of the reaction of C_2H_3 radicals with H_2 is 0.7 s^{-1} which would not affect the fast kinetics of C_4H_6 formation during the above measuring time. Even if our (high) value of $k_1 = 7.1 \times 10^{-18}$ cm^3 molecule^{-1} s^{-1} is used instead, this first-order effective rate constant of the $C_2H_3 + H_2$ is still only 163 s^{-1}.

In the gas chromatographic section of Fahr et al.,[6] their conclusion of approximate equality of the rate constants of reactions 1 and 2 was derived from a comparison of the changes in C_2H_4 and CH_4 yields due to the substitution of He with H_2. These changes (11−27% for CH_4 and 8−21% for C_2H_4) were, on average, a factor of 2 larger than the combined reported[6] uncertainties (1σ) of the total measured yields of these species. Most of the methane and ethylene produced in this system resulted from reactions other than reactions 1 and 2. In addition, a potential contribution to the formation of CH_4 in the presence of molecular hydrogen due to the fast reaction of H atoms formed in reaction 1 with CH_3 radicals (rate constant[10] $\geq 10^{-10}$ cm^3 molecule^{-1} s^{-1}) was neglected in the analysis in ref 6.

As can be seen from Figure 2, the activation energy of the results of Caller and Smith[7] is in reasonable agreement with our extrapolated values of k_1. This is illustrated by shifting the values reported by these authors (which give only a meaningful measure of activation energy since absolute values of k_1 were not measured but assumed) down by a factor of 2.6 to achieve agreement with our absolute values of the rate constants.

Disagreement between our results and the predictions of Tsang and Hampson[9] and Mebel et al.[8] is not surprising. Tsang and Hampson based their recommendation for $k_1(T)$ on the thermochemistry of reactions (1,−1) and on the bond energy − bond order fit to the approximate data of Just et al.[2] for the reverse reaction −1 obtained in a narrow temperature interval (1700−2080 K) by an indirect method. In the calculations of Tsang and Hampson an earlier value for the heat of formation of the vinyl radical $\Delta H_f^\circ{}_{298}(C_2H_3) = 286.2$ kJ mol^{-1} was used which is 13.8 kJ mol^{-1} lower than the one used in our model. Potential uncertainties involved in the analysis were partially reflected in these authors providing an uncertainty factor of 10 for their recommendation.

Mebel et al.[8] calculated the $k_1(T)$ dependence based purely on their ab initio results which included calculating the reaction barrier height at the G2(PU)//QCISD method, which is a modification of the Gaussian-2 (G2) method of Curtiss et al.[33] The G2 method is known to yield heats of formation of small molecules with an accuracy of a few kilocalories per mole and can be expected to give similar or lower accuracy when used to calculate transition-state energies. The disagreement between our experimental results and the prediction of Mebel et al. can be nearly removed by reducing their energy barrier by 5.8 kJ mol^{-1} (Figure 2). The remaining minor disagreement reflects the differences in the transition-state vibrational frequencies (which were adjusted in our model to fit the experimental data) and in the treatment of tunneling. Comparison of our model with the ab initio results of Mebel et al. and with those obtained in the current study (ab initio frequencies, Table 3) show that UMP2/6-31G* or UMP2/6-31G** scaled frequencies of the transition state provide a good approximation for the purpose of calculating the rate constants of reactions (1,−1). Only a relatively minor adjustment of our ab initio frequencies (two lowest frequencies were multiplied by a factor of 1.36) was required to reproduce the experimental data.

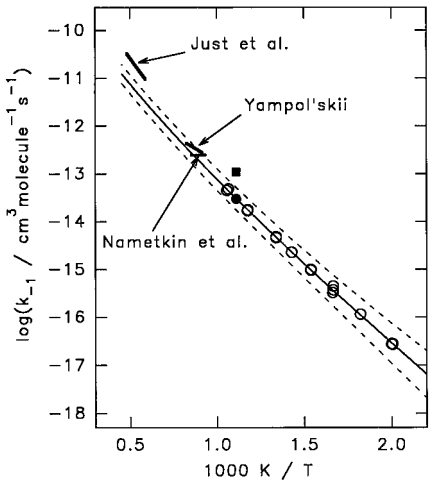

Figure 5. Temperature dependence of k_{-1}: (Open circles) the results of the current study (converted from the k_1 experimental values); (closed square) ref 3; (closed circle) obtained from the data of ref 3 using different values of the rate constants of reference reactions (see text); (heavy lines) Just et al.,[2] Yampol'skii,[4] and Nametkin et al.;[5] (thin solid line) current model; (thin dashed lines) estimated uncertainty limits of the current model.

$H + C_2H_4 \rightarrow C_2H_3 + H_2$ (−1). Yampol'skii[4] and Nametkin et al.[5] studied C_2H_4 pyrolysis in a fluidized bed of powdered quartz at 100 Torr over the temperature ranges 1093−1213 K[4] and 1073−1173 K.[5] Values of k_{-1} were obtained by applying different methods of product analysis. It is unclear to what extent these values were affected by heterogeneous reactions, which could be significant due to a very high surface-to-volume ratio of the powdered quartz. Although the k_{-1} values reported by these authors (Figure 5) are in good agreement with our k_{-1}(T) dependence represented by formula V, it is, most likely, a coincidence.

Just et al.[2] used atomic resonance absorption spectrophotometry (ARAS) to monitor H atoms and infrared spectroscopy to monitor C_2H_4 concentration behind reflected shock waves at temperatures 1700−2200 K. The main purpose of these experiments was to obtain the rate constants of the H-atom-producing channel in the unimolecular decomposition of ethylene. These rate constants were determined with an accuracy of a factor of 2 due to the uncertainty in the H atom signal calibration. Kinetic modeling of the C_2H_4 concentration profiles made it possible to calculate approximate values of k_{-1}, which resulted in the Arrhenius dependence

$$k_{-1}(\text{Just et al.}^2) = 8.3 \times 10^{-9} \times \exp(-(11500\ \text{K})/T)\ \text{cm}^3\ \text{molecule}^{-1}\ \text{s}^{-1} \quad \text{(VI)}$$

shown in Figure 5. As can be seen from the plot, these data

are higher than those obtained from our model (formula V) by approximately a factor of 3.

The values of k_{-1} reported by Just et al. depend on the rate constants of both H-producing and H_2-producing channels of the ethylene thermal decomposition used in the modeling. Although the authors[2] do not provide any estimates of the uncertainties in the values of k_{-1}, they describe their results as approximate and caution that formula VI should not be interpreted in physical terms but considered simply as the expression that best interpolates the experimental data. We, therefore, believe that the difference between our results and those of Just et al. is not very large considering the indirect nature of the values obtained in ref 2.

Our predicted values of k_{-1} at temperatures between 1000 and 3000 K are, on average, lower by a factor of 3 than earlier recommendations of Tsang and Hampson.[9] This disagreement is closely related to the difference between our results and those of Just et al.,[2] since the recommendation of ref 9 was based on a bond energy−bond order fit to the data of ref 2.

Jayaweera and Pacey[3] studied the pyrolysis of ethylene with gas chromatographic analysis of products at 900 K and pressures 150−580 Torr. The rate constant of reaction −1 was determined relative to the product K_6k_7, where K_6 is the equilibrium constant of reaction

$$H + C_2H_4 \rightleftarrows C_2H_5 \quad (6)$$

and k_7 is the rate constant of reaction

$$C_2H_5 + C_2H_4 \rightarrow C_2H_3 + C_2H_6 \quad (7)$$

Extrapolating K_6 values of Brouard et al.[39] to 900 K and taking k_7 from MacKenzie et al.,[40] Jayaweera and Pacey obtain k_{-1}(900 K) = (1.1 ± 0.3) × 10^{-13} cm^3 molecule^{-1} s^{-1} which is 3.6 times higher than our results (Figure 5). K_6 values have been remeasured by Hanning−Lee et al.[41] at 800 K and extrapolation to other temperatures is available via the modeling[41,42] of reaction 6. These newer values of K_6 yield k_{-1}(900 K) = 8.0 × 10^{-13} cm^3 molecule^{-1} s^{-1} from the results of Jayaweera and Pacey if the same k_7 [40] is used. Reaction 7 has been studied by indirect methods only. The values of k_7(900 K) that can be obtained from the literature differ markedly, thus introducing significant uncertainty into the values of k_{-1} obtained from the data of ref 3. For example, if the results of the latest study by Zhang and Back[43] are used in combination with the recommendation of Tsang and Hampson[9] for the rate constant of the $C_2H_5 + H_2 \rightarrow H + C_2H_6$ reaction (reference reaction used by Zhang and Back), we obtain k_7(900 K) = 4.9 × 10^{-17} cm^3 molecule^{-1} s^{-1}. Using this value in interpreting the results of Jayaweera and Pacey yields k_{-1}(900 K) = 3.0 × 10^{-14} cm^3 molecule^{-1} s^{-1} which is in agreement with our values (Figure 5). We therefore conclude that our results on k_{-1} and those of Jayaweera and Pacey are in reasonable agreement considering the combined uncertainties of both studies.

V. Summary

The kinetics of the reactions

$$C_2H_3 + H_2 \rightarrow H + C_2H_4 \quad (1)$$

$$CH_3 + H_2 \rightarrow H + CH_4 \quad (2)$$

have been studied in the temperature ranges 499−947 K (reaction 1) and 646−1104 K (reaction 2) and He densities (6−18) × 10^{16} atoms cm^{-3}. Ethylene was detected as a primary product of reaction 1. Within the above temperature ranges the experimental rate constants can be represented by Arrhenius expressions

$$k_1 = (3.42 \pm 0.35) \times 10^{-12} \times \exp(-(4179 \pm 67\ \text{K})/T)\ \text{cm}^3\ \text{molecule}^{-1}\ \text{s}^{-1} \quad \text{(VII)}$$

$$k_2 = (1.45 \pm 0.18) \times 10^{-11} \times \exp(-(6810 \pm 102\ \text{K})/T)\ \text{cm}^3\ \text{molecule}^{-1}\ \text{s}^{-1} \quad \text{(VIII)}$$

The $k_2(T)$ dependence in combination with the known thermochemistry of the reaction provides the following temperature dependence of the rate constant of the reverse reaction in the same temperature range:

$$k_{-2} = 2.46 \times 10^{-10} \exp(-(6837\ \text{K})/T)\ \text{cm}^3\ \text{molecule}^{-1}\ \text{s}^{-1} \quad \text{(IX)}$$

Both expressions VIII and IX are in good agreement with previous experimental and theoretical studies of reactions 2 and −2.

The potential energy surface and properties of the transition state for reactions (1,−1) were studied by ab initio methods. Experimental and ab initio results of the current study were analyzed and used to create a transition-state model of the reaction. Vibrational frequencies and energy of the transition state were adjusted to reproduce the experimental $k_1(T)$ dependence. The resulting model of the reaction provides the rate constants for both direct (1) and reverse (−1) reactions

$$k_1 = 1.57 \times 10^{-20} T^{2.56} \times \exp(-(2529\ \text{K})/T)\ \text{cm}^3\ \text{molecule}^{-1}\ \text{s}^{-1} \quad \text{(IV)}$$

$$k_{-1} = 8.42 \times 10^{-17} T^{1.93} \times \exp(-(6518\ \text{K})/T)\ \text{cm}^3\ \text{molecule}^{-1}\ \text{s}^{-1} \quad \text{(V)}$$

at 200 K ≤ T ≤ 3000 K. Data on reactions 1 and −1 available in the literature are analyzed and compared with the results of the current study.

Acknowledgment. This research was supported by the Division of Chemical Sciences, Office of Basic Energy Sciences, Office of Energy Research, U.S. Department of Energy under Grant No. DE-FG02-94ER1446. The authors thank Drs. Askar Fahr, Louis J. Stief, and R. Bruce Klemm for helpful discussions and Dr. Philip D. Pacey for the data on the reactions (2,−2).

References and Notes

(1) Warnatz, J. In *Combustion Chemistry*; Gardiner, W. C., Jr., Ed.; Springer-Verlag: New York, 1984.
(2) Just, Th.; Roth, P.; Damm, R. *Symp. (Int.) Combust., [Proc.]* **1977**, *16*, 961.
(3) Jayaweera, I. S.; Pacey, P. D. *Int. J. Chem. Kinet.* **1988**, *20*, 719; **1988**, *20*, 827.
(4) Yampol'skii, Yu. P. *Bull. Acad. Sci. USSR., Div. Chem. Sci.* **1974**, *23*, 532.
(5) Nametkin, N. S.; Shevel'kova, L. V.; Kalinenko, R. A. *Dokl. Chem.* **1975**, *221*, 239.
(6) Fahr, A.; Monks, P. S.; Stief, L. J.; Laufer, A. H. *Icarus* **1995**, *116*, 415.
(7) Callear, A. B.; Smith, G. B. *J. Phys. Chem.* **1986**, *90*, 3229.
(8) Mebel, A. M.; Morokuma, K.; Lim, M. C. *J. Chem. Phys.* **1995**, *103*, 3440.
(9) Tsang, W.; Hampson, R. F. *J. Phys. Chem. Ref. Data* **1986**, *15*, 1087.
(10) Baulch, D. L.; Cobos, C. J.; Cox, R. A.; Esser, C.; Frank, P.; Just, Th.; Kerr, J. A.; Pilling, M. J.; Troe, J.; Walker, R. W.; Warnatz, J. *J. Phys. Chem. Ref. Data* **1992**, *21*, 411.
(11) Laufer, A. H.; Gardner, E. P.; Kwok, T. L.; Yung, Y. L. *Icarus* **1983**, *56*, 560.
(12) Weissman, M. A.; Benson, S. W. *J. Phys. Chem.* **1988**, *92*, 4080.

(13) (a) Slagle, I. R.; Park, J.-Y.; Heaven, M. C.; Gutman, D. *J. Am. Chem. Soc.* **1984**, *106*, 4356. (b) Knyazev, V. D.; Slagle, I. R. *J. Phys. Chem.* **1995**, *99*, 2247.

(14) (a) Russel, J. J.; Seetula, J. A.; Senkan, S. M.; Gutman, D. *Int. J. Chem. Kinet.* **1988**, *20*, 759. (b) Russel, J. J.; Senkan, S. M.; Seetula, J. A.; Gutman, D. *J. Phys. Chem.* **1989**, *93*, 5184. (c) Seakins, P. W.; Pilling, M. J.; Niiranen, J. T.; Gutman, D.; Krasnoperov, L. N. *J. Phys. Chem.* **1992**, *96*, 9847.

(15) Knyazev, V. D.; Slagle, I. R. Submitted for publication in *J. Phys. Chem.*

(16) Knyazev, V. D.; Dubinsky, I. A.; Slagle, I. R.; Gutman, D. *J. Phys. Chem.* **1994**, *98*, 11099.

(17) Rabinowitz, M. J.; Sutherland, J. W.; Patterson, P. M.; Klemm, R. B. *J. Phys. Chem.* **1991**, *95*, 674.

(18) Marquaire, P.-M.; Dastidar, A. G.; Manthorne, K. C.; Pacey, P. D. *Can. J. Chem.* **1994**, *72*, 600.

(19) Baeck, H. J.; Shin, K. S.; Yang, H.; Qiun, Z.; Lissianski, V.; Gardiner, W. C., Jr. *J. Phys. Chem.* **1995**, *99*, 15925.

(20) Slagle, I. R.; Gutman, D. *J. Am. Chem. Soc.* **1985**, *107*, 5342.

(21) Roth, P.; Just, Th. *Ber. Bunsen-Ges. Phys. Chem.* **1975**, *79*, 682.

(22) Frisch, M. J.; Trucks, G. W.; Head-Gordon, M.; Gill, P. M. W.; Wong, M. W.; Foresman, J. B.; Johnson, B. G.; Schlegel, H. B.; Robb, M. A.; Replogle, E. S.; Gomperts, R.; Andres, J. L.; Raghavachari, K.; Binkley, J. S.; Gonzalez, C.; Martin, R. L.; Fox, D. J.; Defrees, D. J.; Baker, J.; Stewart, J. J. P.; Pople, J. A. *Gaussian 92*, Revision E.1; Gaussian, Inc.: Pittsburgh, PA, 1992.

(23) Gonzalez, C.; Schlegel, H. B. *J. Phys. Chem.* **1990**, *94*, 5523.

(24) Schlegel, H. B. *J. Chem. Phys.* **1986**, *84*, 4530.

(25) Schlegel, H. B. *J. Phys. Chem.* **1988**, *92*, 3075.

(26) Pople, J. A.; Scott, A. P.; Wong, M. W.; Radom, L. *Isr. J. Chem.* **1993**, *33*, 345.

(27) Eckart, C. *Phys. Rev.* **1930**, *35*, 1303.

(28) Chao, J.; Zwolinski, B. J. *J. Phys. Chem. Ref. Data* **1975**, *4*, 251.

(29) Chase, M. W., Jr.; Davies, C. A.; Downey, J. R., Jr.; Frurip, D. J.; McDonald, R. A.; Syverud, A. N. JANAF Thermochemical Tables, 3rd ed. *J. Phys. Chem. Ref. Data* **1985**, *14*, Suppl. No. 1.

(30) Pedley, J. B.; Naylor, R. D.; Kirby, S. P. *Thermochemical Data of Organic Compounds*, 2nd ed.; Chapman and Hall: New York, 1986.

(31) Ervin, K. M.; Gronert, S.; Barlow, S. E.; Gilles, M. K.; Harrison, A. G.; Bierbaum, V. M.; DePuy, C. H.; Lineberger, W. C.; Ellison, G. B. *J. Am. Chem. Soc.* **1990**, *112*, 5750.

(32) Berkowitz, J.; Ellison, G. B.; Gutman, D. *J. Phys. Chem.* **1994**, *98*, 2744.

(33) (a) Curtiss, L. A.; Raghavachari, K.; Trucks, G. W.; Pople, J. A. *J. Chem. Phys.* **1991**, *94*, 7221. (b) Kaiser, E. W.; Wallington, T. J. *J. Phys. Chem.* **1996**, *100*, 4111.

(34) Johnston, H. S. *Gas Phase Reaction Rate Theory*; The Ronald Press: New York, 1966.

(35) Bevington, P. R. *Data Reduction and Error Analysis for the Physical Sciences*; McGraw-Hill: New York, 1969.

(36) *Thermodynamic Properties of Individual Substances*; Gurvich, L. V., Veyts, I. V., Alcock, C. B., Eds.; Hemisphere: New York, 1992; Vol. 2, Parts 1 and 2.

(37) Fahr, A.; Braun, W.; Laufer, A. H. *J. Phys. Chem.* **1993**, *97*, 1502.

(38) Fahr, A.; Laufer, A. H. *J. Phys. Chem.* **1988**, *92*, 7229.

(39) Brouard, M.; Lightfoot, P. D.; Pilling, M. J. *J. Phys. Chem.* **1986**, *90*, 445.

(40) MacKenzie, A. L.; Pacey, P. D.; Wimalasena, J. H. *Can. J. Chem.* **1983**, *61*, 2033.

(41) Hanning-Lee, M. A.; Green, N. J. B.; Pilling, M. J.; Robertson, S. H. *J. Phys. Chem.* **1993**, *97*, 860.

(42) Feng, Y.; Niiranen, J. T.; Bencsura, A.; Knyazev, V. D.; Gutman, D.; Tsang, W. *J. Phys. Chem.* **1993**, *97*, 871.

(43) Zhang, H.-X.; Back, M. H. *Int. J. Chem. Kinet.* **1990**, *22*, 21.

JP9606568